Supporting Information

A novel covalent organic framework containing triazine-trithiophene for dual-mode fluorescent and colorimetric detection of Fe^{2+} and Fe^{3+} in water, kale and bovine liver samples

Huaiyi Zhang[a], Zeeshan Ali[a], Wenzhong Hu[b]*, Guang Wang[a,b]*

[a]*Faculty of Chemistry, Northeast Normal University, Changchun 130024, PR China*

[b]*School of Life Sciences, Zhuhai College of Science and Technology, Zhuhai, 519080, P.R. China*

Corresponding author: Guang Wang

Tel: 86+431+85099371;

E-mail：wangg923@nenu.edu.cn (G. Wang)

Corresponding author: Wenzhong Hu

Tel: 86+756+7626318;

E-mail：hwz@dlnu.edu.cn

Contents for Supporting Information

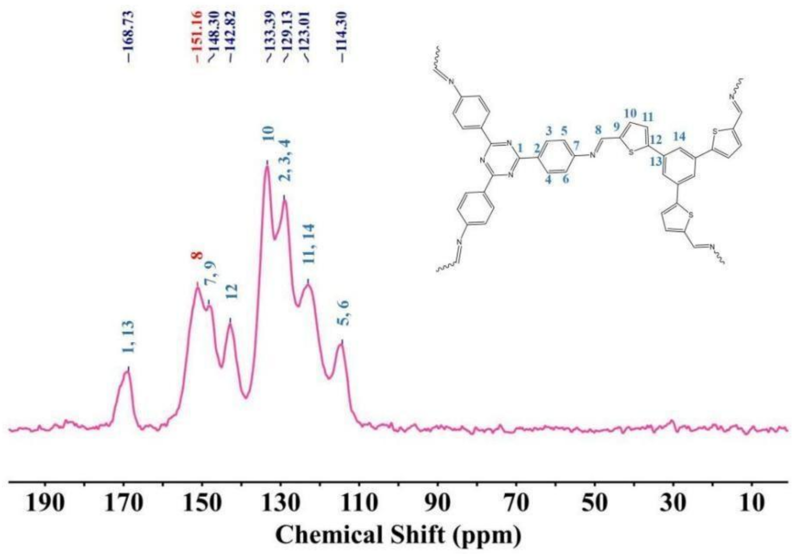

Fig. S1. ^{13}C CP/MAS NMR of BTTC-TTA COF

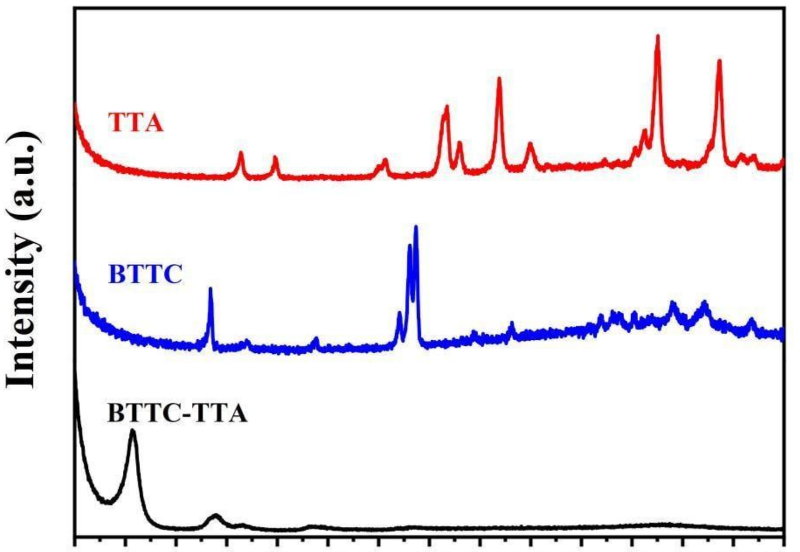

Fig. S2. PXRD patterns of BTTC, TTA and BTTC-TTA COF.

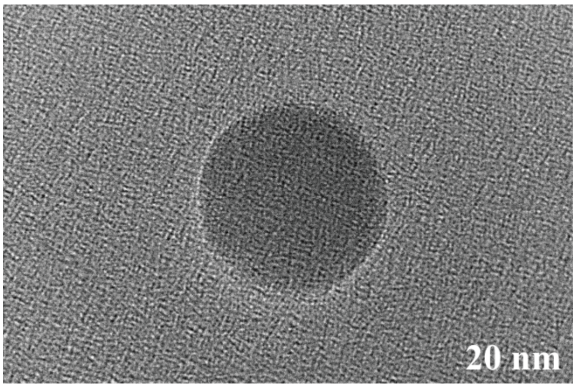

Fig. S3. HR-TEM image of BTTC-TTA COF.

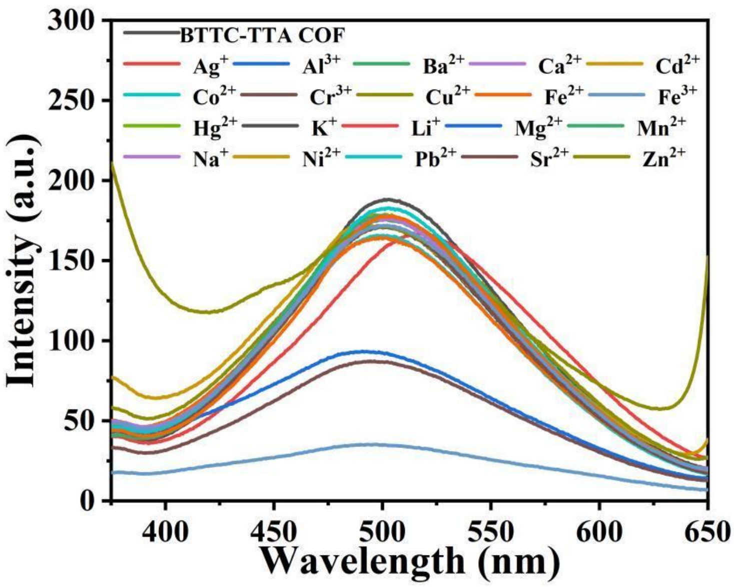

Fig. S4. Fluorescence emission spectra of BTTC-TTA COF (3 mL, 0.05 g/L) upon the addition of different metal ions (30 μL, 20 mM) in ethanol.

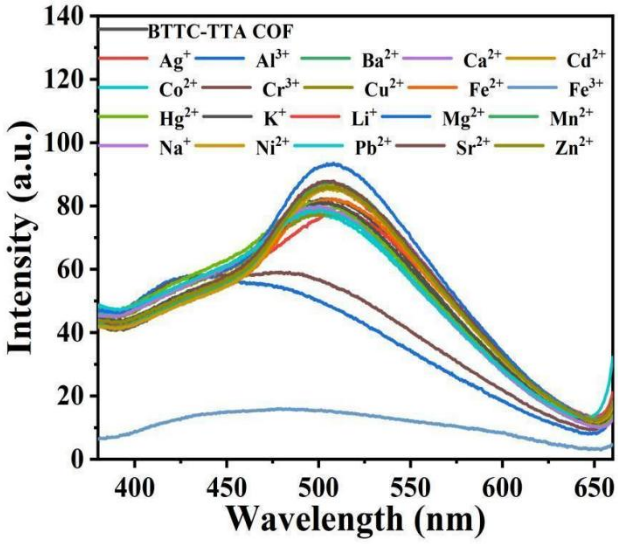

Fig. S5. Fluorescence emission spectra of BTTC-TTA COF (3 mL, 0.05 g/L) upon the addition of different metal ions (30 μL, 20 mM) in methanol.

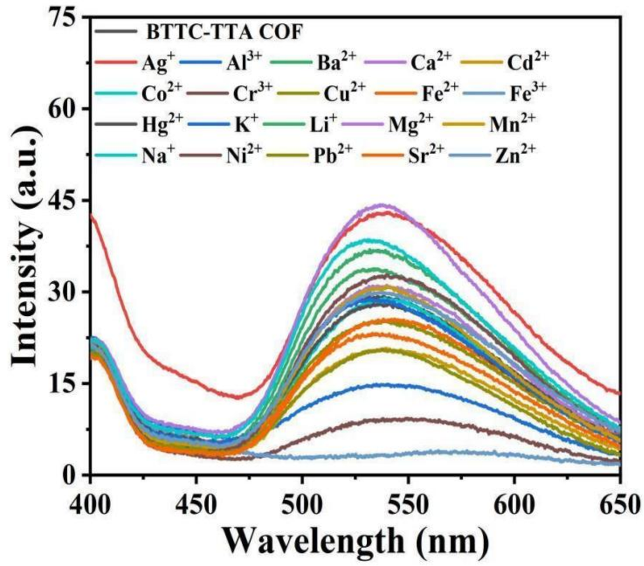

Fig. S6. Fluorescence emission spectra of BTTC-TTA COF (3 mL, 0.05 g/L) upon the addition of different metal ions (30 μL, 20 mM) in water.

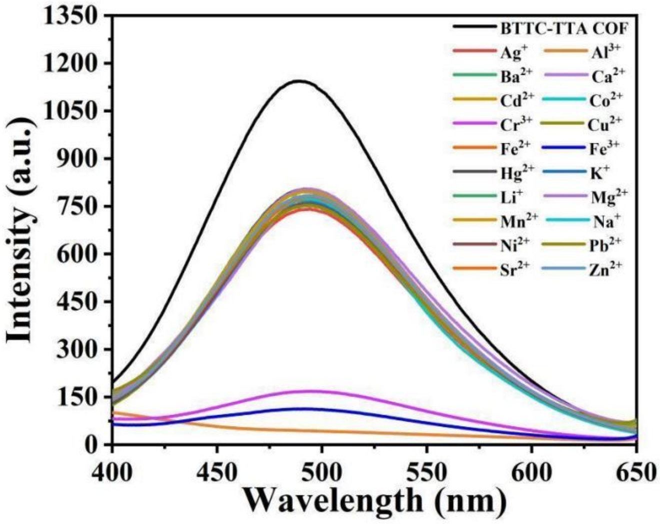

Fig. S7. Fluorescence emission spectra of BTTC-TTA COF (3 mL, 0.05 g/L) upon the addition of different metal ions (30 μL, 20 mM) in CH_3CN.

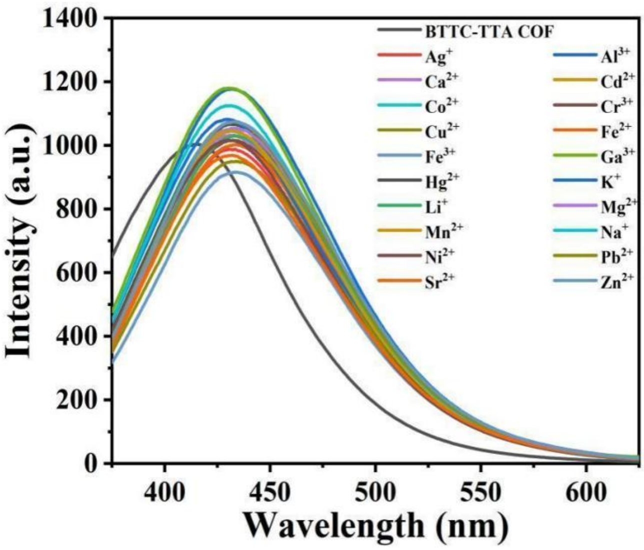

Fig. S8. Fluorescence emission spectra of BTTC-TTA COF (3 mL, 0.05 g/L) upon the addition of different metal ions (30 μL, 20 mM) in 1,4-dioxane.

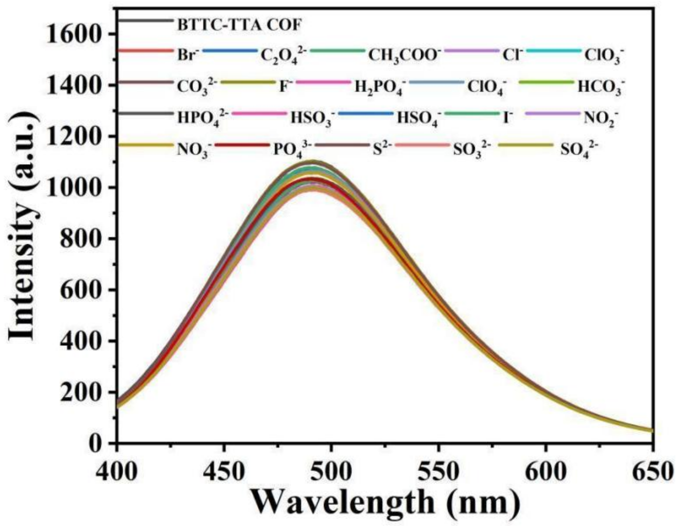

Fig. S9. Fluorescence emission spectra of BTTC-TTA COF (3 mL, 0.05 mg/mL) in DMF after the addition of different anions (30 μL, 20 mmol/L) in DMF (λ_{ex} = 350 nm)

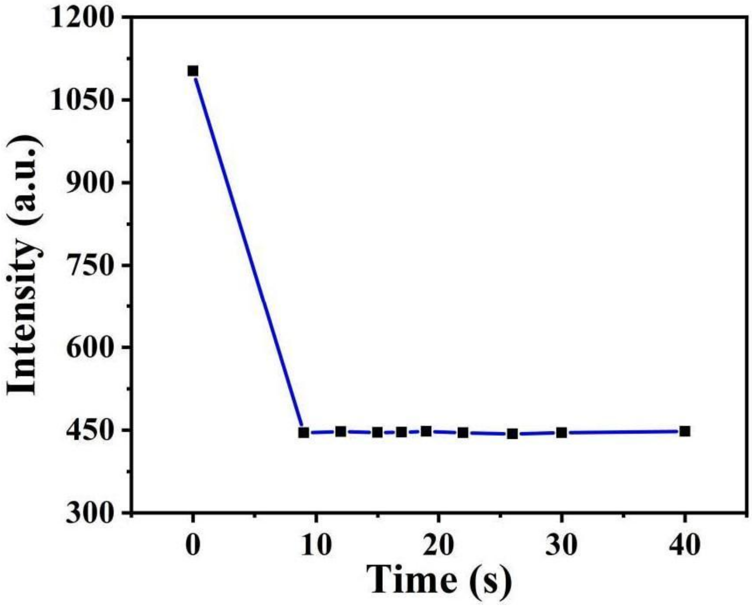

Fig. S10. Change in the fluorescence intensity of BTTC-TTA COF (3 mL, 0.05 g/L) with time after the addition of Fe^{2+} (30 μL, 20 mM) in DMF (λ_{ex} = 350 nm).

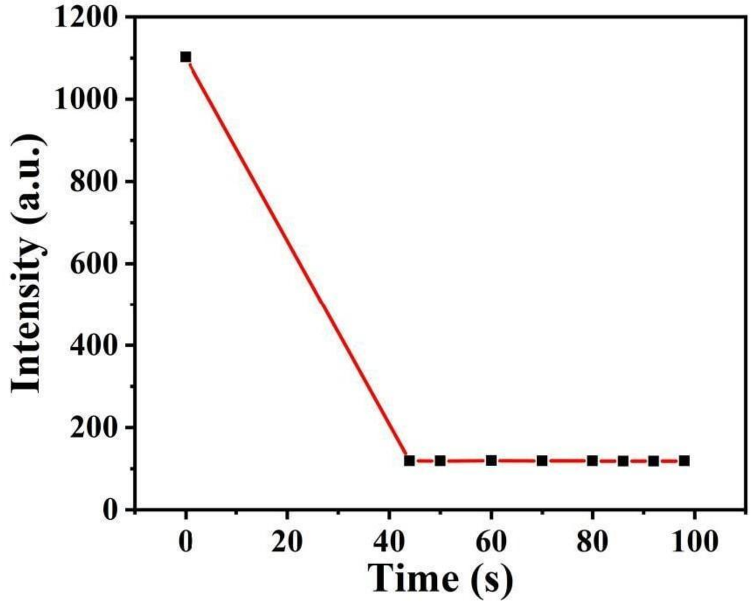

Fig. S11. Change in the fluorescence intensity of BTTC-TTA COF (3 mL, 0.05 g/L) with time after the addition of Fe^{3+} (30 μL, 20 mM) in DMF (λ_{ex} = 350 nm).

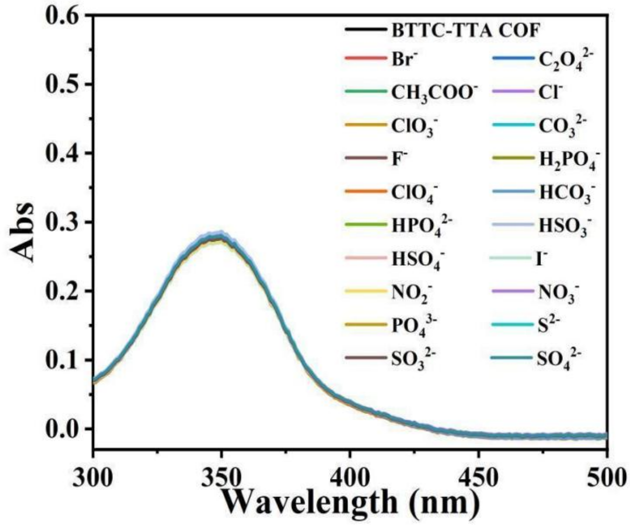

Fig. S12. The UV-vis absorbance spectra of BTTC-TTA COF (3 mL, 0.05 mg/mL) in DMF after the addition of different anions (30 μL, 20 mmol/L).

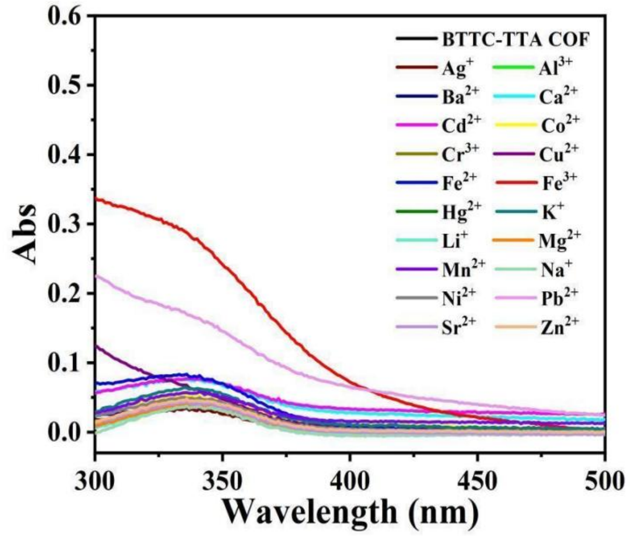

Fig. S13. The UV-vis absorbance spectra of BTTC-TTA COF (3 mL, 0.05 mg/mL) in ethanol after the addition of different metal ions (30 μL, 20 mmol/L).

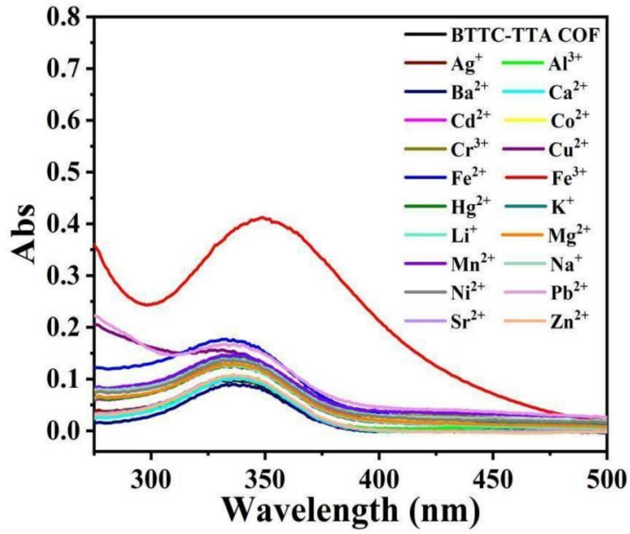

Fig. S14. The UV-vis absorbance spectra of BTTC-TTA COF (3 mL, 0.05 mg/mL) in methanol after the addition of different metal ions (30 μL, 20 mmol/L).

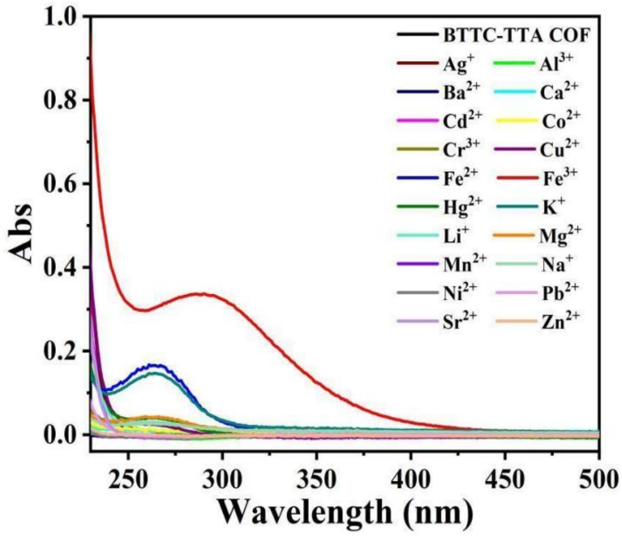

Fig. S15. The UV-vis absorbance spectra of BTTC-TTA COF (3 mL, 0.05 mg/mL) in H_2O after the addition of different metal ions (30 μL, 20 mmol/L).

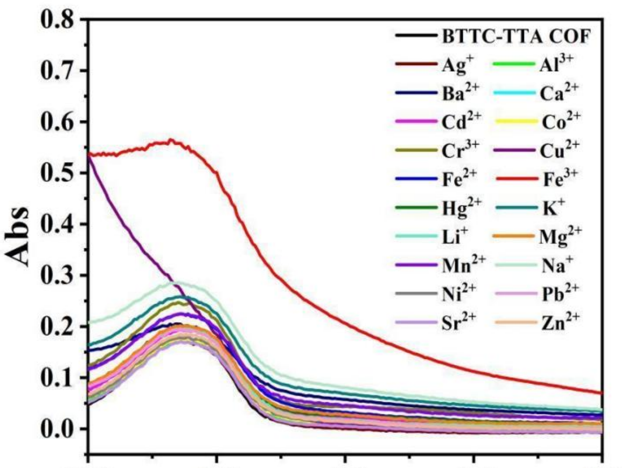

Fig. S16. The UV-vis absorbance spectra of BTTC-TTA COF (3 mL, 0.05 mg/mL) in 1,4-dioxane after the addition of different metal ions (30 μL, 20 mmol/L).

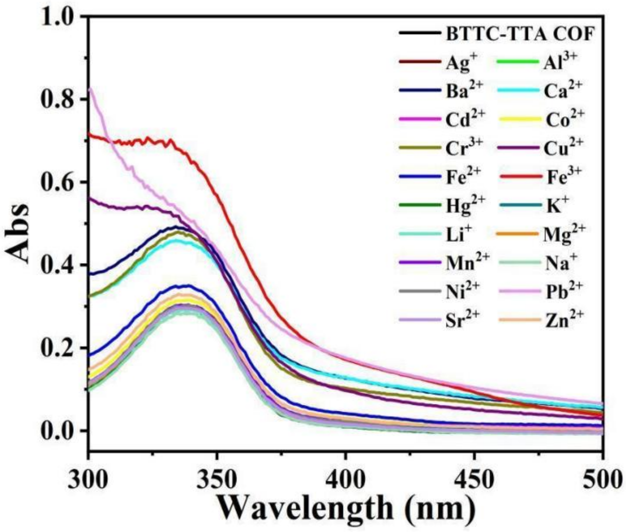

Fig. S17. The UV-vis absorbance spectra of BTTC-TTA COF (3 mL, 0.05 mg/mL) in CH_3CN after the addition of different metal ions (30 μL, 20 mmol/L).

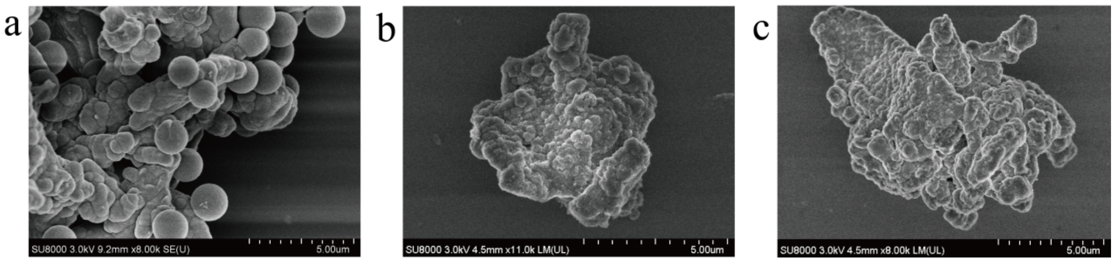

Fig. S18. SEM images of (a) BTTC-TTA COF, (b) BTTC-TTA COF@Fe^{2+} and (c) BTTC-TTA COF@Fe^{3+}.

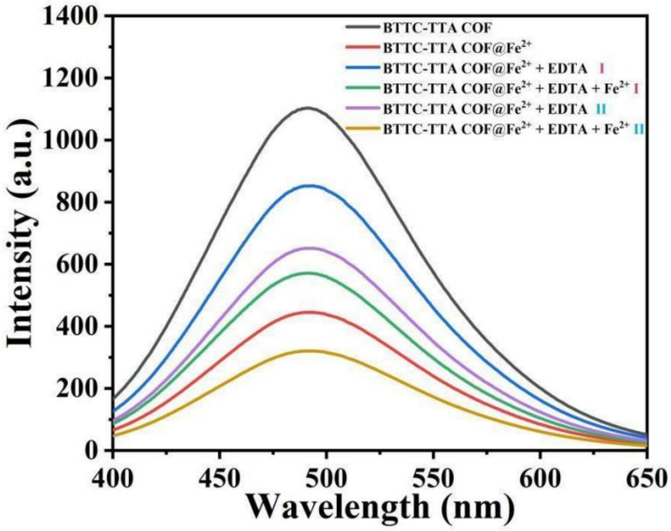

Fig. S19. The fluorescence spectra of BTTC-TTA COF in DMF in the presence and absence of Fe^{2+} ions and EDTA. "I" indicates the first addition of EDTA and Fe^{2+} (both 60 μL, 20 mM) to a solution of BTTC-TTA COF and Fe^{2+}, "II" indicates the second addition of EDTA and Fe^{2+} (both 60 μL, 20 mM) to the above solution.

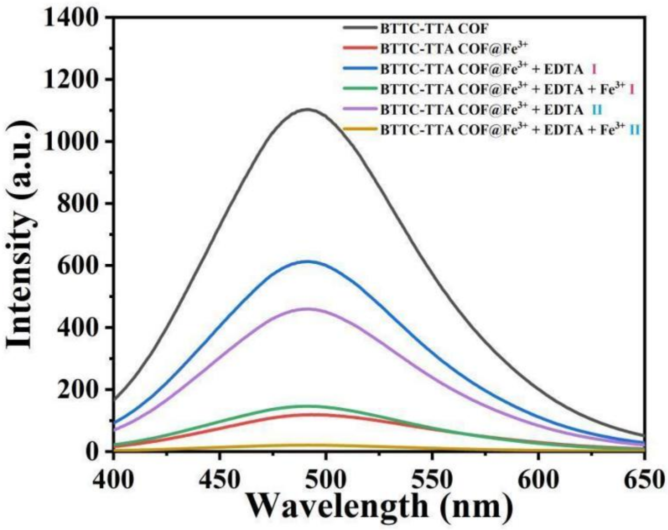

Fig. S20. The fluorescence spectra of BTTC-TTA COF in DMF in the presence and absence of Fe^{3+} ions and EDTA. "I" indicates the first addition of EDTA and Fe^{3+} (both 60 μL, 20 mM) to a solution of BTTC-TTA COF and Fe^{3+}, "II" indicates the second addition of EDTA and Fe^{3+} (both 60 μL, 20 mM) to the above solution.

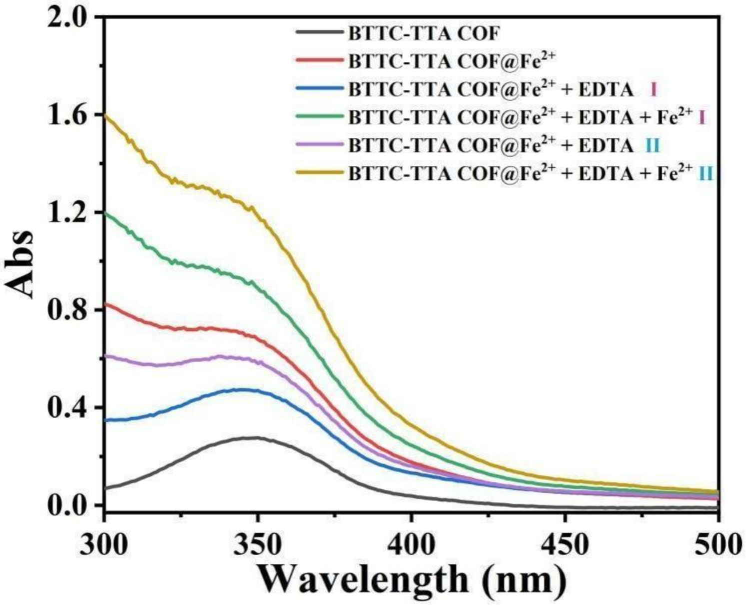

Fig. S21. The UV-vis absorbance spectra of BTTC-TTA COF in DMF in the presence and absence of Fe^{2+} ions and EDTA. "I" indicates the first addition of EDTA and Fe^{2+} (both 60 μL, 20 mM) to a solution of BTTC-TTA COF and Fe^{2+}, "II" indicates the second addition of EDTA and Fe^{2+} (both 60 μL, 20 mM) to the above solution.

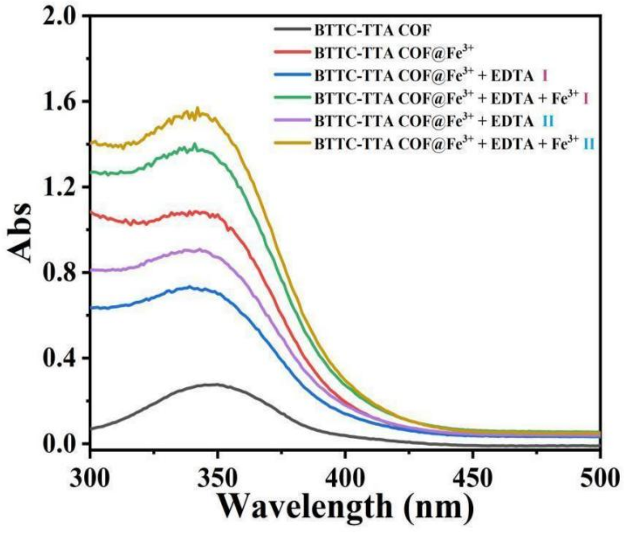

Fig. S22. The UV-vis absorbance spectra of BTTC-TTA COF in DMF in the presence and absence of Fe^{3+} ions and EDTA. "I" indicates the first addition of EDTA and Fe^{3+} (both 60 μL, 20 mM) to a solution of BTTC-TTA COF and Fe^{3+}, "II" indicates the second addition of EDTA and Fe^{3+} (both 60 μL, 20 mM) to the above solution.

Fig. S23. The color changes of DMF with the addition of Fe^{2+} and Fe^{3+} (30 μL, 20 mM) under naked eye.

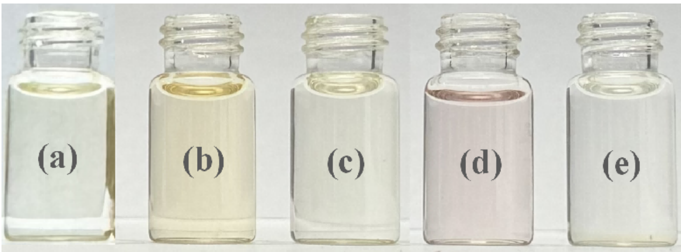

Fig. S24. (a) The color of BTTC-TTA COF in DMF. (b) and (c) The color changes of BTTC-TTA COF@Fe^{2+} in DMF in the absence and presence EDTA, respectively. (d) and (e) The color changes of BTTC-TTA COF@Fe^{3+} in DMF in the absence and presence EDTA, respectively.

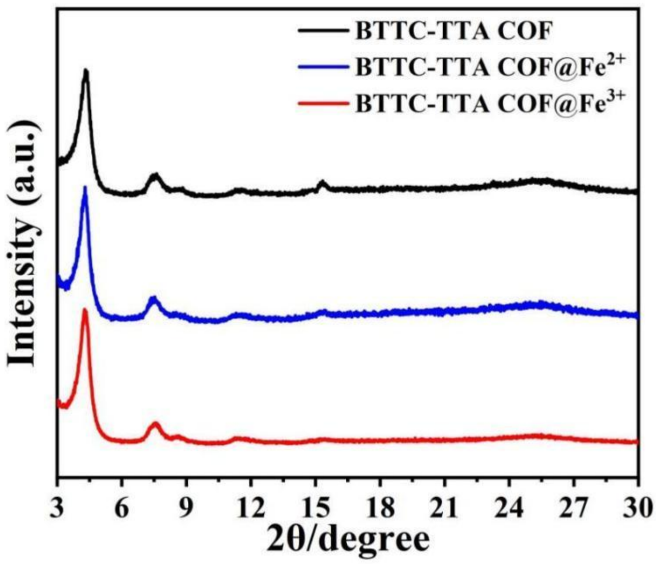

Fig. S25. Comparative PXRD patterns of BTTC-TTA COF, BTTC-TTA COF@Fe^{2+} and BTTC-TTA COF@Fe^{3+}.

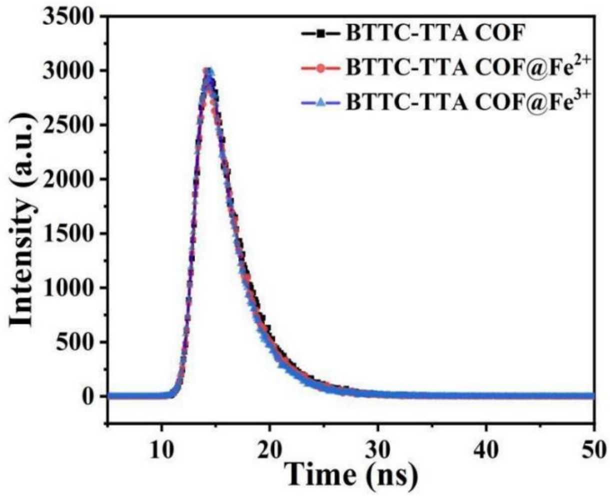

Fig. S26. Fluorescence decay curves of BTTC-TTA COF, BTTC-TTA COF@Fe^{2+}, BTTC-TTA COF@Fe^{3+}.

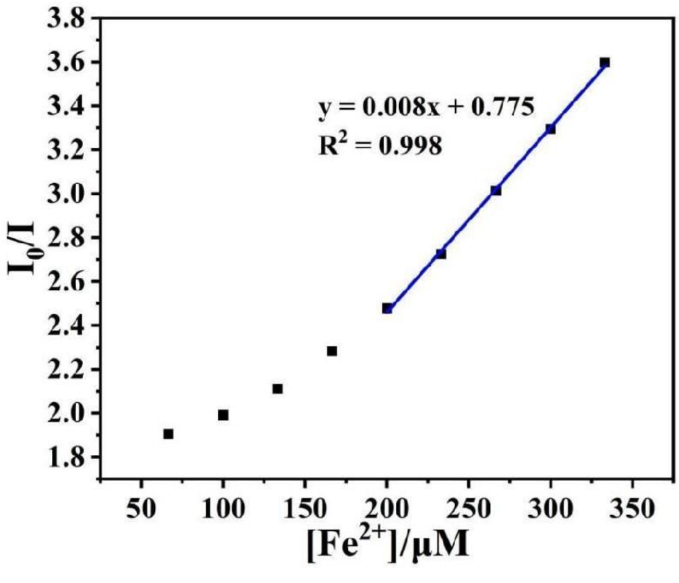

Fig. S27. Fluorescence intensity ratio (I/I_0) of BTTC-TTA COF at 492 nm with the concentration of Fe^{2+} (where I_0 and I stand for the fluorescence intensity in the absence and presence of metal ions.)

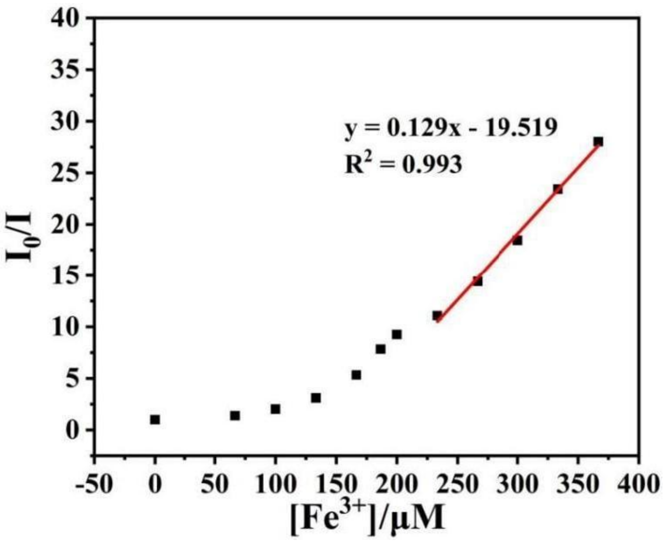

Fig. S28. Fluorescence intensity ratio (I/I_0) of BTTC-TTA COF at 492 nm with the concentration of Fe^{3+} (where I_0 and I stand for the fluorescence intensity in the absence and presence of metal ions.)

Table S1. Comparison of detection limits of the reported Fe^{2+}/Fe^{3+} fluorescent sensors.

Fluorescent materials	LOD	Application	Reference
SS1	55.00 μM (Fe^{2+}) 36.64 μM (Fe^{3+})	filter paper-based analyses	1
SS2	22.15 μM (Fe^{2+}) 14.33 μM (Fe^{3+})	filter paper-based analyses	1
Sensor 1	7.78 μM (Fe^{2+}) 6.95 μM (Fe^{3+})	water and living cell imaging	2
CQDs	6.50 μM (Fe^{2+}) 2.50 μM (Fe^{3+})	water	3
BTTC-TTA COF	4.51 μM (Fe^{2+}) 0.79/ 8.94 μM (Fe^{3+})	water, kale and bovine liver samples	this work

Table S2. Comparison of detection limits of the reported Fe^{2+}/Fe^{3+} colorimetric sensors.

Colorimetric materials	LOD	Reference
Terminalia chebula	43.7 μM (Fe^{2+}) 60.8 μM (Fe^{3+})	4
Probe 3	4.35 μM (Fe^{2+})	5
T-CDs	0.13 μM (Fe^{2+}) 2.78 μM (Fe^{3+})	6
$MoSe_2$@Fe	1.97 μM (Fe^{3+})	7
BHMN	3.10 μM (Fe^{3+})	8
BTTC-TTA COF	2.61 μM (Fe^{2+}) 1.56 μM (Fe^{3+})	this work

Table S3. The detected iron ions concentration of real samples.

Samples	Concentration/ μM
Tap water	< LOD (Fe^{2+}) 2.54 μM (Fe^{3+})
Drinking water	< LOD (Fe^{2+}) 3.23 μM (Fe^{3+})
Kale extract	5.10 μM (Fe^{2+}) 3.67 μM (Fe^{3+})
Bovine liver extract	7.24 μM (Fe^{2+}) 82.46 μM (Fe^{3+})

References

1 S. Sasan, T. Chopra, A. Gupta, D. Tsering, K. K. Kapoor and R. Parkesh, ACS Omega, 2022, 7, 11114.

2 X. Gong, H. Zhang, N. Jiang, L. Wang and G. Wang, Microchem. J., 2019, 145, 435.

3 P. Siahcheshm and P. Heiden, J. Photochem. Photobiol. A: Chem., 2023, 435, 114284.

4 S. Sen, T. Singh, J. Im, D. Debnath and G. Biswas, J. Anal. Sci. Technol., 2022, 13, 39.

5 R. Nagarajan, E. Kamaraj, C.-H. Kim and K. H. Lee, Talanta Open, 2022, 6, 100143.

6 T. Jiang, J. Huang and G. Ran, Anal. Sci., 2023, 39, 325.

7 L. Lin, D. Chen, C. Lu and X. Wang, Microchem. J., 2022, 177, 107283.

8 S. Moon, M. Lee and C. Kim, Chem. Select, 2022, 7, e202201353.